Active Cavity Radiometric Scale, International Pyrheliometric Scale, and Solar Constant

RICHARD C. WILLSON

Jet Propulsion Laboratory, Pasadena, California 91109

The active cavity radiometer type II, a new and accurate standard detector, has been developed for the absolute measurement of optical radiant flux. The active cavity radiometric scale (ACRS), defined by the active cavity radiometer (ACR), and the international pyrheliometric scale (IPS), defined by a U.S. standard angstrom pyrheliometer, have been compared in recent experiments. Simultaneous measurements of solar irradiance demonstrated an average systematic difference between the two scales of 2.2%, the measurements on the ACRS exceeding those on the IPS. An analytical study of the sensitivity of the ACR to sources of experimental error is presented. The uncertainty in the ACRS is found to be less than ±0.5% at the one solar constant level relative to the absolute scale based on fundamental physical principles. In August 1968 two ACR's measured the solar irradiance at an altitude of 25 km in a balloon-flight experiment. The solar-constant value derived from this measurement was $H_0 = 137.0$ mw/cm^2.

Scales for the measurement of radiant energy are established with respect to fundamental physical concepts by standard detectors or standard emitters of radiant energy. Establishment of a scale of radiometry by a standard emitter usually involves the irradiance of a suitable (nonstandard) detector by a high-temperature blackbody source of thermal radiation. If the properties of the source and the characteristics of the radiation transfer between the source and the detector are well known, the detector can be calibrated relative to the radiation scale defined by the operation of the source. The calibrated detector can then be used to measure other radiation fields and to report the results on the radiometric scale defined by its calibration. The radiant exitance of the blackbody source can be predicted very accurately from physical theory. One of the principal sources of error in this method is the uncertainty in the radiative transfer of source energy to the detector.

The definition of a radiometric scale with a standard detector does not suffer from the propagation uncertainty. A standard detector is so designed that its interaction with an incident radiation field can be accurately predicted from a knowledge of its instrumental parameters, along with the basic framework of physical laws that define the fundamental physics of radiation processes.

The active cavity radiometric scale (ACRS) is defined by the active cavity radiometer type II (ACR II), a standard detector. The cavity radiometer was developed at the Jet Propulsion Laboratory (JPL) [*Haley*, 1964; *Plamondon and Kendall*, 1965; *Kendall* 1968; *Willson*, 1969] to calibrate the vacuum radiation environments of the JPL space environment simulators. The original cavity radiometer has been enclosed in a vacuum case and modified for operation by automatic electronic circuitry. The resulting radiometric device is referred to as the active cavity radiometer type II.

The international pyrheliometric scale (IPS) of 1956 was defined by an international radiation conference held in that year. In 1957 it was adopted by the World Meteorological Organization as the international radiometric scale. It is a compromise scale, chosen as an average between the prominent radiometric scales in use at that time [*Crommelynk and Dongniaux*, 1970]. It was primarily intended to facilitate comparisons of solar-irradiance measurements on an international basis. The primary instrument used to define the IPS is the Stockholm angstrom pyrheliometer. In the U.S. the Eppley Laboratory of Newport, Rhode Island,

maintains standard Eppley-Angstrom pyrheliometers that are calibrated relative to the Stockholm standard.

The accuracy of a scale of radiometry, relative to the absolute scale based on fundamental physical concepts, depends on the uncertainties inherent in the method employed to define the scale. Therefore an upper limit to the accuracies of the ACRS and the IPS should be demonstrable through an analysis of the sensitivities of the ACR and the angstrom pyrheliometer to common sources of experimental uncertainty. This approach will be meaningful in establishing the uncertainty of the ACRS relative to the absolute scale, since every ACR is used as an independent standard detector. The absolute uncertainty of the IPS is not so accessible to this analytical approach, however, since the Eppley-Angstroms used to reproduce the IPS in the experimental phase of this project were not used as standard detectors, but as transfer standards, calibrated relative to a 'standard' European angstrom. A definitive analysis of the IPS absolute uncertainty would require knowledge of the specific set of instrumental parameters (and their associated indeterminancies) for the 'standard' angstrom pyrheliometer.

The ACR research program in basic radiometry at JPL has progressed through four phases. The first phase was the development of the ACR; the second, the analytical determination of the absolute uncertainty of the ACRS under different measurement conditions; the third, the experimental comparison of the ACRS and the IPS; and the fourth, an experimental determination of the solar constant, on the ACRS, from solar irradiance measurements made by two ACR's in a high-altitude (25 km) balloon-flight experiment.

ACTIVE CAVITY RADIOMETER (ACR)

Description of the Active Cavity Radiometer Type II (ACR II)

The ACR has several significant advantages in relation to most other standard detectors. The first and most significant advantage results from the use of a cavity detecting element. The uncertainty of the cavity aperture's absorptance for radiant flux is decreased by an order of magnitude relative to that of a flat detecting surface [*Syndor*, 1970; *Sparrow and Jonsson*, 1963; *Sparrow*, 1965]. The second advantage is the precise thermal control by a 'thermal guard' of the environment surrounding the detecting element. The thermal guard and cavity are maintained at nearly the same temperature; thus, uncertainties due to radiative or conductive heat exchange between them are minimized or eliminated. A third advantage of the ACR is its automatic operation by compact solid-state electronic circuits. This feature facilitates remote operations in any environment and thus makes the ACR available for a wide range of absolute radiant flux measurements.

The construction of the ACR-II is shown in Figure 1. The radiometer has a low-mass, silver, cavity-detecting element (C). Its interior surface is coated with a material having a high absorptance for the solar spectral distribution. Surrounding the cavity is the 'thermal guard' (G) and heat sink (GS). Platinum resistance

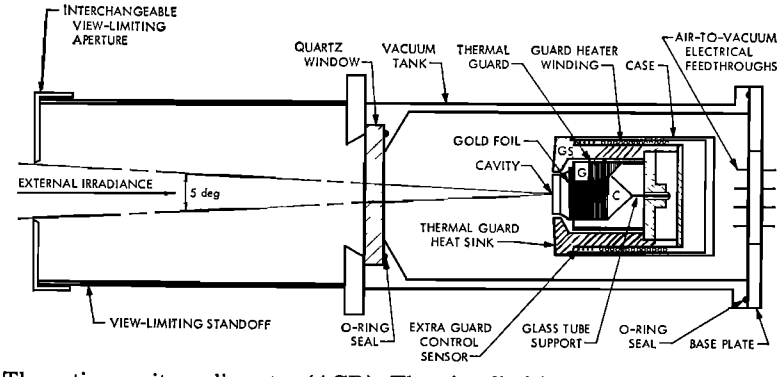

Fig. 1. The active cavity radiometer (ACR). The view-limiting standoff is used in comparing the ACRS and the IPS.

sensors are wound on both the cavity and the thermal guard. A guard heater is wound on the outer surface of the guard heat sink. A gold foil wrapping covers the cavity winding.

The cavity and guard are actively controlled at the same constant temperature by automatic solid-state electronic circuits, hence the name active cavity radiometer. With the guard platinum winding as a sensor, the guard servo maintains the guard temperature by regulating the dc power supplied to its heater. The cavity temperature is controlled by another servo having the cavity platinum winding as both sensor and heater (see Figure 2). Preliminary temperature calibration assures equality of guard and cavity temperatures.

The ACR was developed for operation in the hard vacuum of the JPL space environment simulators. For operation in nonvacuum environments, the radiometer has been enclosed in a small portable vacuum chamber. The source of irradiance to be measured is viewed through a quartz window. The vacuum enclosure's environmental infrared contributions to the measured irradiance are eliminated by shuttering the irradiance on the source side of the quartz window.

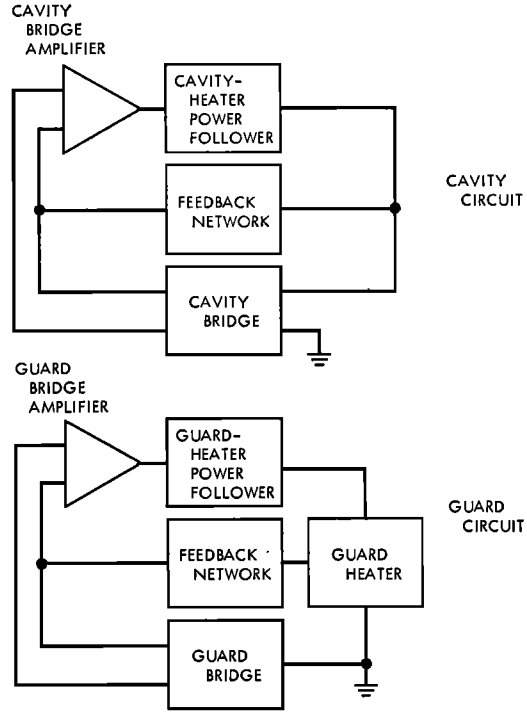

Fig. 2. Operational schematic diagram of the ACR II electronics.

Derivation of the ACR II Working Equation

General nature of the working equation. The ACR-II is an electrical substitution calorimeter operated at a constant temperature (164°C). Its cavity aperture is, therefore, a source of constant exitance. In the absence of external irradiance (shutter-closed phase), electrical heating and environmental infrared irradiance from the vacuum enclosure provide the necessary power to balance the radiative losses and maintain the cavity at the preselected temperature. When an external source of radiation (shutter-open phase) is viewed, the power supplied by the electronics automatically decreases by an amount proportional to the external source's irradiance of the cavity aperture. Absolute irradiance measurements are made by a determination of the electrical power supplied to maintain constant cavity temperature in the two phases of each measurement, i.e., with and without the external radiation field. This mode of operation assumes that the only significant difference between the two phases of measurement is the presence or absence of the external source's irradiance. Of course, this assumption is an idealization, and, to the extent that it is unrealized, errors are introduced into the measurement. The magnitude and direction of these errors will be treated later. From the previous discussion we would expect the form of the working equation to be

$$H = C[P_{ec} - P_{eo}] \tag{1}$$

where

H is the measured irradiance.
C is the constant of proportionality.
P_{ec} is the cavity heater power without an external radiation field (shutter closed).
P_{eo} is the cavity heater power with an external radiation field (shutter open).

The constant of proportionality is the term that facilitates the absolute measurement of radiation by a standard detector. It contains instrumental parameters, such as the detector area and absorptance, whose specifications determine the interaction between the radiometer and irradiant fluxes.

The functional relationship between the ACR and the irradiance it is measuring can be developed through an equilibrium power-balance analysis. The detailed character of the standard detector constant will become apparent when the functional relationship (working equation) is put into the form of equation 1.

Equilibrium power-balance relationships. The sum of the power inputs to and losses from the ACR cavity with the shutter closed are

$$\sum P_{in} = P_{ec} + \rho_{ir}P_{out} + P_e + P_{cgc} \quad (2)$$

$$\sum P_{out} = (\epsilon_c A_c + \epsilon_a A_a)\sigma T^4 \quad (3)$$

The sum of the cavity power inputs and losses with the shutter open are

$$\sum P_{in}' = P_{eo} + \rho_{ir}P_{out}' + P_e' + P_{cgc}' + \tau H(\alpha_c A_c + \alpha_a A_a) + \rho H(\alpha_c A_c + \alpha_a A_a) \quad (4)$$

$$\sum P_{out}' = (\epsilon_c A_c + \epsilon_a A_a)\sigma T_c'^4 \quad (5)$$

where

P_{ec}, P_{eo} are the cavity electrical powers.

$\rho_{ir}P_{out}$ is the fraction of the radiant flux emitted by the radiometer and reflected back into its own aperture.

ρ_{ir} is the reflectance factor for cavity exitance.

P_e is the environmental infrared radiative input to the cavity aperture from the interior surface of the vacuum enclosure.

P_{cgc} is any net radiative or conductive power input to the cavity from the guard due to small departures from radiometer isothermality.

ϵ_c is the effective emittance of the cavity aperture.

A_c is the cavity aperture area.

ϵ_a is the effective emittance of the external surface of the cavity through the narrow annulus between the cavity and the guard.

A_a is the area of the annulus surrounding the cavity aperture.

T_c is the cavity temperature.

σT_c^4 is the blackbody exitance at temperature T_c.

σ is the Stefan-Boltzmann constant (5.6697×10^{-9} mw/cm^2/°K^4)

$\tau H(\alpha_c A_c + \alpha_a A_a)$ is the direct power input to the cavity due to the irradiance being measured.

$\rho H(\alpha_c A_c + \alpha_a A_a)$ is the power input due to irradiance reflected from the front surface of the guard to the vacuum enclosure or the quartz window and back into the cavity aperture and annulus.

τ is the effective transmittance of the quartz window for the irradiance. (This quantity will be a function of spectral distribution.)

α_a is the effective absorptance of the external cavity surface for the irradiance entering the annular clearance.

H is the irradiance on the source side of the instrument window due to the radiation field to be measured.

ρ is the reflectance factor for the irradiance (H).

The primed quantities denote shutter-open values. All measurements are made with the ACR at thermodynamic equilibrium, which requires that $\Sigma P_{in} = \Sigma P_{out}$ and $\Sigma P'_{in} = \Sigma P'_{out}$. These conditions and equations 2 through 5 yield expressions for P_{ec} and P_{eo} in terms of other known ACR parameters.

Differential measurement. Measurement of the amounts of electrical power required to maintain constant exitance at the cavity aperture in the shutter-closed (P_{ec}) and shutter-open (P_{eo}) phases constitutes one cycle of differential measurement. The difference between P_{ec} and P_{eo} provides the first form of the functional relationship between the ACR and the irradiance it is measuring (H). This relationship can be solved for the irradiance in terms of known properties of the radiometer and the two measured values of electrical power, P_{ec} and P_{eo}.

$$H = [(\tau + \rho)(\alpha_c A_c + \alpha_a A_a)]^{-1}\{[P_{ec} - P_{eo}] + (P_e - P_e') - (\epsilon_c A_c + \epsilon_a A_a)\sigma(T_c^4 - T_c'^4) + \rho_{ir}(P_{out} - P_{out}') + (P_{cgc} - P_{cgc}')\} \quad (6)$$

The last four terms of equation 6 are ACR temperature-difference terms. They can be shown to have the form of products of constants and the temperature differences of the vacuum enclosure, cavity, and guard between

the shutter-closed and shutter-open phases of measurement. The differential mode of measurement minimizes radiometer dependence on these terms, which are identified as environmental irradiance (P_e, P_e'), the cavity's absolute temperature (T_c, T_c'), the reflected cavity exitance ($\rho_{tr}P_{out}$, $\rho_{tr}P_{out}'$), and the conductive and radiative exchanges between the guard and cavity (P_{cgc}, P_{cgc}').

Theoretically the operation of the ACR reduces the differential temperature terms in equation 6 to zero. This reduction is not achievable in practice, but the observed differences between theoretical and practical operation are small. The reflectance factor (ρ) can be made small by proper instrument design. This factor and the differential temperature terms can then be treated as perturbations to the theoretical working equation

$$H = [\tau(\alpha_c A_c + \alpha_a A_a)]^{-1}[P_{ec} - P_{eo}] \qquad (7)$$

Comparison with equation 1 shows the standard detector constant to be the first term on the right-hand side of equation 7. It contains the quartz-window transmittance and the cavity aperture and annulus absorptances and areas.

Error Analysis of the ACR II

The accuracy with which the ACR defines the absolute radiometric scale can be determined by an error analysis of the complete working equation. ACR measurements of irradiance depend only on the measured or computed values of the ACR parameters. The net ACRS uncertainty will be equal to the combination of the parametric uncertainties dictated by the form of equation 6.

The conventional representation of random uncertainty, the standard deviation, will be taken as the criterion for specifying the ACRS uncertainty. In terms of the standard deviations of the ACR parameters, the uncertainty of the ACRS is then

$$U(H) = \pm\left\{\sum_i \left[\frac{\partial H}{\partial \xi_i} S(\xi_i)\right]^2\right\}^{1/2} \qquad (8)$$

where $U(H)$ is the absolute uncertainty of the measured irradiance H and $S(\xi_i)$ is the standard deviation of the parameter ξ_i.

$U(H)$ has been computed as a function of irradiance by using equations 6 and 8 and the parametric values from Table 1. A graphical representation of the results is shown in Figure 3. For levels of irradiance greater than 85 mw/cm² the ACRS is uncertain by less than ±0.5% relative to the absolute radiometric scale defined by fundamental physical laws.

TABLE 1. Characteristic Values of ACR II Parameters and Their Associated Indeterminancies

Parameter	Symbol	Value	Uncertainty (±)
Quartz-window transmittance*	τ	0.925	0.0025
Effective cavity absorptance	α_c	0.9958	0.002
Cavity aperture area, cm²	A_c	1.0128	0.0018
Effective annulus absorptance	α_a	0.5	0.1
Annulus area, cm²	A_a	0.0118	0.0025
Effective cavity emittance	ϵ_c	0.9862	0.002
Effective annulus emittance	ϵ_a	0.5	0.1
Stephan-Boltzmann constant, mw/cm²/°K⁴	σ	5.6697×10^{-9}	0.0007×10^{-9}
Cavity mean temperature, °K	T_c	436.7	0.05
Guard mean temperature, °K	T_g	436.7	0.05
Cavity heater voltage, volts	$V_{c,0}$	25.0	0.005
Cavity heater resistance, ohms	R_c	648.8	0.5
Solar reflectance factor	ρ	0.0004	0.0002
Cone-guard conductance, μw/°K	K	50.0	10.0
Cavity external surface area, cm²	$\langle A_c \rangle$	7.5	0.25
Emittance, cavity external surface	$\langle \epsilon_c \rangle$	0.10	0.05
Infrared reflectance factor	ρ_{ir}	0.0004	0.0002
Infrared emittance, guard internal surface	ϵ_g	0.10	0.05
Vacuum case temperature, °K	T_e	300.0	1.0

* Function of the spectral distribution of the irradiance. This value corresponds to the experimentally measured value for the solar-spectral irradiance at the JPL Table Mountain Observatory, site of the ACRS-IPS comparisons described later.

EXPERIMENTAL COMPARISONS OF ACRS AND IPS

Two experimental intercomparisons were made in 1968 of the radiometric scales defined by the ACR and the angstrom pyrheliometer. The basis for the experiment was a synchronous comparison of solar irradiance measurements made by the two instruments. The tests were conducted at the solar test site of the JPL Table Mountain Observatory. The observatory is situated in the Angeles National Forest, 60 miles southeast of Pasadena, California, at an elevation of 2.25 km.

The first comparison was conducted during May 1968. Two ACR's and two Eppley-Angstrom pyrheliometers were operated in close proximity. One of the two ACR's is shown in Figure 4. The Eppley-Angstrom pyrheliometers used were serial numbers 8420 and 9000. Number 8420, a primary U.S. standard, was operated by a representative of the Eppley Laboratory of Newport, Rhode Island, to reproduce the IPS. Number 9000 is a secondary instrument, owned by JPL, calibrated relative to number 8420.

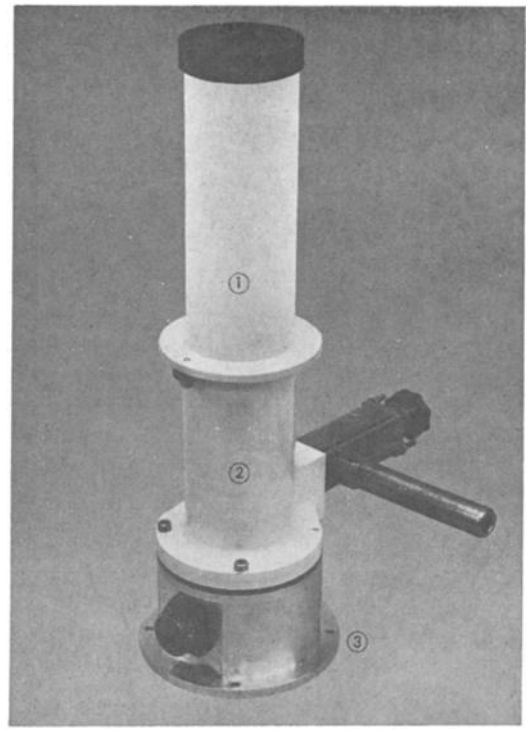

Fig. 4. View of an ACR. (1) View-limiting assembly, (2) vacuum enclosure containing the radiometer sensor, (3) base plate and standoff.

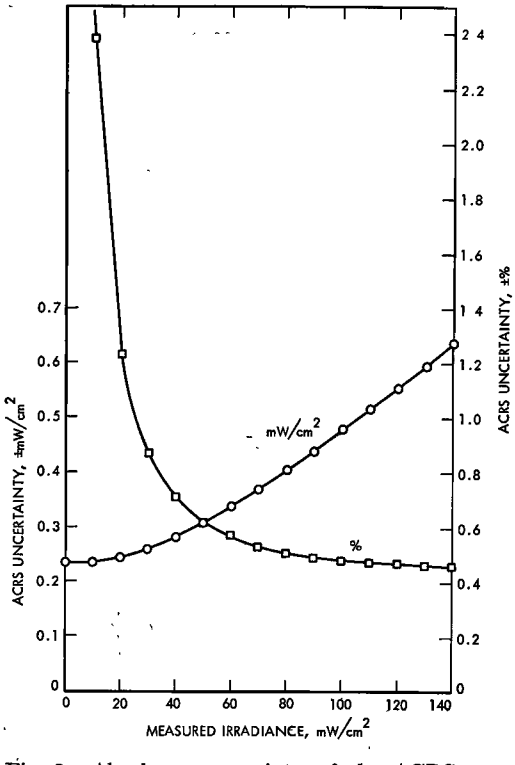

Fig. 3. Absolute uncertainty of the ACRS as a function of irradiance.

The second scale comparison took place in September 1968. Two ACR's, mounted in the balloon-flight payload described in the next section were used to define the ACRS. Eppley-Angstrom pyrheliometer 9000 was operated by an Eppley representative to reproduce the IPS.

Instrumental field of view can be an important factor in the intercomparison of radiometers when significant atmospheric aerosol scattering is present. The ACR has a circular detector geometry and is used with a circular field of view. The Eppley-Angstrom pyrheliometer has a rectangular detecting surface and a rectangular field of view that, when little aerosol scattering is present, is equivalent to a 5° to 6° circular field of view [*Angstrom and Rhode*, 1966]. Several circular apertures providing fields of view ranging from 5° to 10° were tried with the ACR's to evaluate the experimental sensitivity to this parameter. On the days when data were taken, the differences observed between

measurements made within this range did not exceed the (±0.5%) ACR experimental uncertainties indicative of a 'turbidity parameter' of less than $m\beta = 0.05$ [*Schöne,* 1966]. Circumsolar irradiance for fields of view less than 5° would be nearly equally included by both instruments, since the Eppley-Angstrom field of view was 4.4 × 10.6° [*Angstrom and Rhode,* 1966], and the field of view of the ACR's was 5° for all data utilized in the comparisons.

The first Table Mountain comparison test using Eppley-Angstrom pyrheliometer 8420 and ACR 1 is summarized in Table 2. The solar irradiances are average values for 20-min observation periods. Each period represents eight individual Eppley-Angstrom measurements and from 10 to 20 individual ACR measurements. The per cent scale difference (PSD) is defined as

$$\text{PSD} = [1 - (H_{\text{ANG}}/H_{\text{ACR}})] \times 10^{-2} \qquad (9)$$

where H_{ANG} is the Eppley-Angstrom measured irradiance and H_{ACR} is the ACR measured irradiance. The average value of the per cent scale difference for the first test was +2.1% with a standard deviation of ±0.12%.

The second Table Mountain comparison test, summarized in Table 3, presents the results obtained by comparing Eppley-Angstrom pyrheliometer 9000 and ACR 2. The solar irradiances in the table are average values for 3- to 5-min observation periods. The average value of the per cent scale difference for the second Table Mountain test was +2.2% with a standard deviation of ±0.04%.

The weighted average value of the per cent scale difference for the two Table Mountain tests was determined by weighting the values for each test by the total number of measurements in each experiment. The resultant average value of the per cent scale difference is

$$\langle \text{PSD} \rangle = +2.2 \pm 0.055\% \qquad (10)$$

The absolute uncertainty of the ACRS at the 100-mw/cm² irradiance level was shown to be less than ±0.5% under the Table Mountain measurement conditions (see Figure 3). The absolute scale difference (ASD) is then

$$\text{ASD} = +2.2 \pm 0.5\% \qquad (11)$$

It has been suggested that forward scattering by atmospheric aerosols near the apparent solar position (the solar aureole) might have significantly different effects on Eppley-Angstrom pyrheliometers and ACR's, thereby contributing to the ASD. The ASD should depend on the optical thickness of atmospheric aerosols if the aureole was a significant factor during the Table Mountain tests. The total atmospheric optical thickness varied with solar zenith distance over the range of 0.75 to 1.25 air mass throughout the two 1968 comparison experiments. A least-squares analysis of the set of ASD versus air-mass data showed a weak 0.02% per air-mass dependency, insufficient to explain the 2.2% ASD. The per cent scale difference as a function of air mass for the five days of comparisons in the May and September 1968 tests is shown in Figure 5.

Four ACR's and the prototype Pacrad [*Ken-*

TABLE 2. Table Mountain Comparison Test 1*

Date of Observation	Period of Observation	Time, PDT	Angstrom Pyrheliometer 8420 Average Irradiance, mw/cm²	ACR 1 Average Irradiance, mw/cm²	Scale Difference, %
May 10, 1968	1	0945–1005	96.7	99.0	2.3
	2	1020–1040	98.2	100.1	1.9
	3	1100–1120	99.4	101.5	2.1
	4	1140–1200	98.5	99.9	1.4
	5	1220–1240	96.9	99.1	2.2
	6	1305–1315	95.2	97.1	2.0
May 11, 1968	7	0935–0955	95.6	98.0	2.4
	8	1020–1040	98.0	100.6	2.6
	9	1110–1130	98.6	100.9	2.3

* Experimental comparison of the average solar irradiances measured over 20-min periods by Eppley-Angstrom pyrheliometer 8420 and the JPL ACR 1 on May 10 and 11, 1968, at Table Mountain, California.

dall, 1969] were used to define the ACRS during the two Table Mountain comparisons. The results for the Pacrad are reported elsewhere [*Kendall,* 1970]. Each of these instruments was operated as a standard detector, calibrated not by comparison with each other, but by independent measurements of the standard detector parameters of each instrument. In the first test ACR's 1 and 2 and the Pacrad were operated simultaneously. The results reported in Table 2 are for ACR 1. The average measurements of all three instruments agreed to within less than ±0.25%. In the second test ACR's 2 and 4 and the Pacrad were used simultaneously to define the ACRS. Again the average measurements of all three instruments agreed to within ±0.25%.

The 2.2% ASD is clearly common to the radiometric techniques employed at JPL, and not to any particular instrument. Although the

TABLE 3. Table Mountain Comparison Test 2*

Date of Observation	Observation Period	Time, PDT	Angstrom Pyrheliometer 9000 Average Irradiance, mw/cm²	ACR 2 Average Irradiance, mw/cm²	Scale Difference, %
September 23, 1968	1	1500	102.6	104.9	2.2
	2	1515	101.4	103.7	2.2
	3	1530	101.2	103.3	2.0
September 24, 1968	4	1000	101.7	103.7	1.9
	5	1015	102.2	104.9	2.6
	6	1020	103.1	105.4	2.2
	7	1030	103.5	106.1	2.4
	8	1045	104.0	106.4	2.3
	9	1051	104.2	107.1	2.7
	10	1100	104.8	107.2	2.2
	11	1105	104.8	107.2	2.2
	12	1145	106.0	108.6	2.4
	13	1200	106.1	108.6	2.3
	14	1245	105.9	108.8	2.7
	15	1300	106.1	108.4	2.1
	16	1422	104.3	106.9	2.4
	17	1430	103.9	106.4	2.4
	18	1440	102.6	105.5	2.6
September 25, 1968	19	1450	102.5	104.7	2.1
	20	0950	99.4	101.4	2.0
	21	1002	100.5	102.7	2.1
	22	1015	101.1	103.3	2.1
	23	1027	101.8	104.2	2.3
	24	1035	102.4	104.4	1.9
	25	1105	103.4	105.3	1.8
	26	1120	103.8	106.0	2.0
	27	1140	104.3	106.2	1.8
	28	1148	104.3	106.6	2.2
	29	1157	104.3	106.4	2.0
	30	1210	104.3	106.8	2.3
	31	1246	104.5	106.7	2.1
	32	1300	104.2	106.4	2.0
	33	1315	104.3	106.3	1.9
	34	1332	103.6	105.8	2.1
	35	1344	103.6	105.6	1.9
	36	1354	102.7	105.4	2.5
	37	1410	102.2	104.2	1.9
	38	1420	101.8	103.8	1.9
	39	1430	101.1	103.6	2.4

* Experimental comparison of the average value of solar irradiances measured over 3- to 5-min periods by the Eppley-Angstrom pyrheliometer 9000 and the ACR 2.

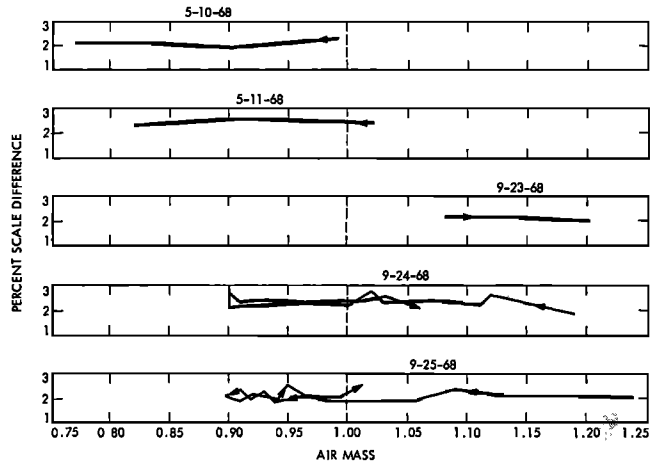

Fig. 5. ACRS-IPS scale differences as functions of the absolute air mass $M = (p/p_0)$ sec Z. Arrows indicate data track throughout test.

ACR's II and the Pacrad both employ cavity detectors and are electrical substitution devices, their configurations and modes of operation are very different. The 2.2% scale difference has consistently manifested itself through comparisons of all ACR's and the Pacrad with the IPS.

ACR SOLAR CONSTANT MEASUREMENT

1968 ACR II Balloon Flight

The ACR's high absolute accuracy and automatic operation make it an ideal instrument for the remote measurement of optical radiant fluxes. The use of the ACR for a direct measurement of the solar constant in a high-altitude or extra-atmospheric experiment has a singular advantage relative to previous efforts: until the ACR ballon flight of August 1968, a standard detector had never been employed in a high-altitude measurement of the solar constant.

The opportunity to use the ACR in a balloon-flight experiment arose in 1968 as a part of the JPL solar cell standardization program. Two ACR's were built into a compact flight package that interfaced with a top-mounted balloon solar-tracker assembly. The essential features of the instrument (shown in Figure 6) are the two ACR's mounted inside their individual vacuum chambers, the rotating shutter assembly, the cryogenic adsorption pump (for maintaining vacuum during flight), and the temperature-controlled electronics bay that mounts directly on the solar tracker.

The 1968 ACR payload contained a rotating shutter wheel with three open positions and a rotating filter wheel with six filter positions, both operated by six-position geneva mechanisms. Five of the filter wheel positions contained long-wave passing filters designed to provide spectral data for the experimental solar cells mounted below. The sixth filter wheel position contained no filter; the absence of a filter facilitated direct measurement of the solar irradiance. Timing circuits, synchronized with the telemetry system, advanced the shutter wheel every 6 min and the filter wheel every 12 min; thus each radiometer-filter combination was repeated every 72 min.

Launch occurred on August 20, 1968, at New Brighton, Minnesota. A stable float altitude of 25 ($\pm$0.5) km was achieved before 1000 CST and sustained until after 1400 CST. More than 40 independent determinations of the filtered and unfiltered solar irradiance at 25 km were made and telemetered to the ground receiving station.

Balloon-Flight Data

The two ACR's each made four unfiltered solar-irradiance measurements during the 25-km float period. These solar irradiances, measured by the ACR's inside their vacuum chambers, are known with little uncertainty (less than $\pm$0.5%) relative to the absolute scale. They have been attenuated, however, by both the earth's atmosphere and the ACR quartz win-

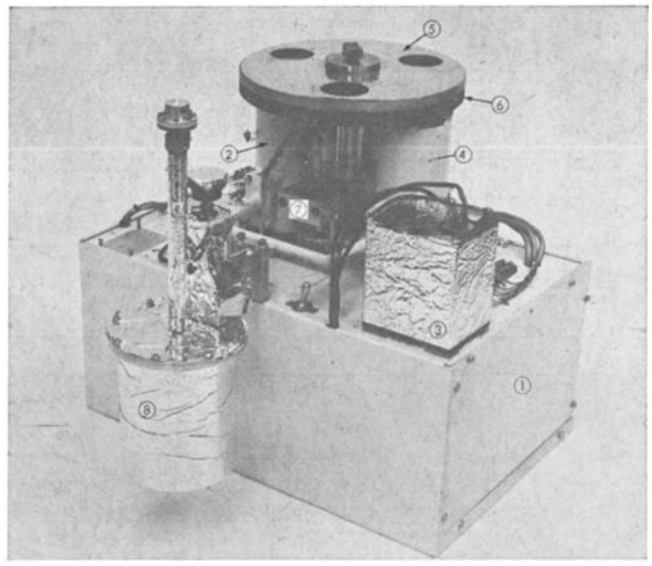

Fig. 6. 1968 ACR balloon-flight payload. (1) Base plate and protective box enclosing the radiometer electronic circuitry, (2, 4) vacuum enclosures in which active cavity radiometers 2 and 4 are located, (3) power supply (dc-dc converter), (5) chopper wheel, (6) filter wheel, (7) twin geneva mechanisms for operation of chopper and filter wheels, (8) cryogenic vacuum pump.

dows. Computation of the solar constant requires an accurate knowledge of the attenuating properties of both.

The transmissivities of the ACR quartz windows were carefully determined before and after the flight by using double-beam spectrophotometers. An average difference of 2.85% due to contamination of the vacuum side of the windows during flight was observed. This window transmission uncertainty was the largest single source of error for the experiment.

Determining the transmittance of the earth's atmosphere for solar radiation is a complex problem. In the troposphere or low stratosphere variable water-vapor and aerosol concentrations frustrate accurate transmittance computations. With the exception of ozone, however, the attenuation of the remaining atmosphere above 25 km is due only to permanent, constant mixing ratio gases and totals less than 3%. The uncertainty in computing the 25-km attenuation is thought to be less than $\pm 10\%$, resulting in a net contribution to the uncertainty of the solar-constant value of less than $\pm 0.3\%$.

The data required to compute the atmospheric transmittance were taken from two sources. Extinction optical thicknesses [*Elterman*, 1965] account for Rayleigh and aerosol scattering and ozone absorption. Selective absorption by the constant mixing ratio gases CO_2, O_2, CH_4, and N_2O was accounted for by using research data [*Houghton*, 1963] for computing the equivalent widths of the gases' significant vibration-rotation bands in the solar-spectral range.

Computation of the Solar Constant

The solar-constant value derived from each independent ACR total irradiance measurement contains three basic corrections. The first is for the transmission of the ACR quartz window, the second is for the attenuation of the remaining earth's atmosphere, and the third is a correction of the results to an earth-sun distance of 1 AU.

The solar spectral range was divided into 37 bands for computing the window and atmospheric effects. Numerous narrow bands were used in wavelength ranges where the window or atmosphere has selective adsorption features, and relatively few broad bands were used where absorption varied slowly with wavelength. Five solar-spectral models [*Arvesen et al.*, 1969; *Gast*, 1965; *Labs and Neckel*, 1968; *Thekae-*

TABLE 4. Properties of the Weighted, Average Solar-Spectral Model and the Earth's Atmosphere above 25 km Used to Compute the Solar Constant from the ACR Balloon Data

Spectral Bands		Parameters				
λ min, μ	λ max, μ	β_i (25 km → ∞)	$H_{0,i}$, mw/cm²	$H_{25,i}$, mw/cm²	τ_A	$H_{0,i} - H_{25,i}$, mw/cm²
0.000	0.275	25.4120	0.588	0.000	0.000	0.588
0.275	0.290	12.8440	0.373	0.000	0.000	0.373
0.290	0.310	1.2510	1.069	0.220	0.206	0.848
0.310	0.330	0.1320	1.515	1.283	0.847	0.233
0.330	0.350	0.0260	1.844	1.785	0.968	0.060
0.350	0.370	0.0150	2.050	2.012	0.981	0.038
0.370	0.390	0.0120	2.036	2.005	0.985	0.031
0.390	0.425	0.0090	5.398	5.337	0.989	0.061
0.425	0.475	0.0060	9.561	9.489	0.992	0.072
0.475	0.525	0.0080	9.632	9.535	0.990	0.097
0.525	0.575	0.0140	9.392	9.228	0.982	0.164
0.575	0.630	0.0180	9.690	9.473	0.978	0.218
0.630	0.685	0.0090	8.605	8.508	0.989	0.097
0.685	0.695	0.0040	1.470	1.462	0.995	0.007
0.695	0.750	0.0020	7.482	7.463	0.997	0.019
0.750	0.770	0.0040	2.500	2.487	0.995	0.013
0.770	0.850	0.0000	8.916	8.916	1.000	0.000
0.850	0.950	0.0000	9.035	9.035	1.000	0.000
0.950	1.260	0.0000	18.564	18.564	1.000	0.000
1.260	1.280	0.0003	0.894	0.893	1.000	0.000
1.280	1.400	0.0000	5.112	5.112	1.000	0.000
1.400	1.500	0.0040	0.954	0.949	0.995	0.005
1.500	1.900	0.0010	10.496	10.483	0.999	0.013
1.900	2.100	0.0170	0.758	0.742	0.979	0.016
2.100	2.500	0.0000	4.038	4.038	1.000	0.000
2.500	2.670	0.0000	0.778	0.778	1.000	0.000
2.670	2.700	0.0000	0.126	0.126	1.000	0.000
2.700	2.800	0.3150	0.366	0.246	0.672	0.120
2.800	2.850	0.0000	0.161	0.161	1.000	0.000
2.850	3.000	0.0000	0.441	0.441	1.000	0.000
3.000	3.200	0.0000	0.467	0.467	1.000	0.000
3.200	3.500	0.0050	0.522	0.519	0.994	0.003
3.500	3.800	0.0000	0.378	0.378	1.000	0.000
3.800	4.175	0.0000	0.337	0.337	1.000	0.000
4.175	4.425	1.0940	0.169	0.043	0.251	0.127
4.425	5.000	0.0030	0.274	0.273	0.996	0.001
5.000		0.0100	0.694	0.686	0.987	0.009

kara et al., 1969], the fifth being a weighted average model, were used to compute atmospheric and window transmittances and solar-constant values. The spectral bands, the extinction optical thicknesses, the flux in each band, and the atmospheric attenuation are shown in Table 4 for the averaged spectral model. The equivalent widths for O_2, CO_2, NH_4, and N_2O are fitted into the appropriate bands, and the band extinction optical thickness is adjusted accordingly. The values in this table correspond to an earth-sun distance of 1 AU and a solar zenith angle of 37.6°.

In Table 4 the minimum and maximum wavelengths of the 37 spectral bands are given in microns. The extinction optical thicknesses ($\beta_{25,i}$) are those of *Elterman* [1965], with the exception of the bands 0.75–0.77 μ, 1.40–1.50 μ, 1.90–2.10 μ, 2.7–2.8 μ, 3.2–3.5 μ, 4.175–4.425 μ, 4.425–5.00 μ, and 5.00–100.00 μ, which are augmented by the equivalent widths of O_2, CO_2, CO_2, CO_2, CH_4, CO_2, N_2O, and CO_2 absorption bands, respectively. The attenuation due to other strong absorption bands beyond 5 μ has little effect on the atmospheric transmission because of the small amount of solar flux in this wavelength range.

The solar spectrum at 25 km is computed

under the assumption that the Bougher-Lambert law, using the previously defined extinction optical thicknesses, holds to good approximation for the atmospheric attenuation in each of the 37-wavelength bands. The irradiance in the ith band at 25 km is

$$H_{25,i} = H_{0,i} \exp - [\beta_i \sec Z] \quad (12)$$

where $H_{0,i}$ is the extra-atmospheric irradiance in ith band, β_i is the extinction optical thickness of the ith band, and Z is the zenith angle of sun.

The total irradiance at 25 km is

$$H_{25} = \sum_{i=1}^{37} H_{25,i} \quad (13)$$

The effective transmittances of the ACR quartz windows and the atmosphere are functions of spectral distribution. Both have absorption features in the ultraviolet and infrared that produce different over-all transmittances for spectral models with different amounts of UV and IR flux. The UV and IR, the most difficult spectral ranges to measure accurately, are the wavelength ranges in which the various solar-spectral models differ most. Therefore the quartz window and atmospheric model produce an ACR measurement and solar-constant computation sensitivity to the solar-spectral model.

The effective transmittances of the ACR windows are computed for each model from the derived 25-km solar irradiance.

$$\tau_w = \sum_{i=1}^{37} H_{25,i}\tau_{w,i} \Big/ \sum_{i=1}^{37} H_{25,i} \quad (14)$$

where τ_w is the effective window transmittance and $\tau_{w,i}$ is the window transmissivity. (The concept of the effective transmittance has its root in the law of the mean for integrals. Here we approximate the two integrals by finite sums.) The effective atmospheric transmittance can similarly be defined as

$$\tau_A = \sum_{i=1}^{37} H_{0,i} \exp - [\beta_i \sec Z] \Big/ \sum_{i=1}^{37} H_{0,i} \quad (15)$$

where τ_A is the effective atmospheric transmittance. The ACR irradiance measurements (H) can now be used to compute the total solar irradiance, both at 25 km and outside the atmosphere, in absolute units on the active cavity radiometric scale (ACRS). The 25-km irradiance is

$$H_{25} = H\tau_w^{-1} \quad (16)$$

The solar constant, including the earth-sun distance correction, is

$$H_0 = HR^2(\tau_w\tau_A)^{-1} \quad (17)$$

where H_0 is the solar constant and R is the earth-sun distance (in AU). The values of τ_w, τ_A, H_{25}, and H_0 have been computed for both ACR's (2 and 4) for each solar-spectral model.

Discussion of the Computations

Table 5 is a summary of the results of the 1968 ACR balloon flight. The average measured irradiance (H) represents the average of the four measurements of irradiance, inside the ACR vacuum cases, made by each radiometer. The standard deviation of the average measured irradiance ($S(H)$) provides an indication of the consistency of the H data.

The transmittance of the quartz windows (τ_w) is computed for each solar-spectral model by using equation 14. The value of τ_w depends on the spectral distribution of the model and the solar-zenith angle at the time of each ACR measurement. It does not depend on the model solar constant. The τ_w of Table 5 is the average of the transmittance of a clean window measured before the flight and the contaminated window measured after the flight. Since it is not possible to specify the degree of contamination effective at the time of each measurement, the averaged transmittance value is used, and an uncertainty for this value equal to half the difference of pre- and post-flight transmittances is assigned. By using the average τ_w, the total solar irradiance at 25 km is computed from equation 16.

The atmospheric transmittance (τ_A), computed from equation 15, is dependent on the spectral distribution of each solar-spectral model and the secant of the solar-zenith angle at the time of each measurement. The transmittances τ_A and τ_w are averages for the four ACR measurements.

The solar-constant values for each solar-spectral model and each radiometer are computed by using equation 17. The solar-radius vector at the time of the flight was 1.01177 AU. The

TABLE 5. Results of 1968 ACR Balloon Flight for the Two Solar Spectrum Models

Parameters	Symbol	Arvesen Model		Gast Model		Labs and Neckel Model		Goddard Space Flight Center Model		Weighted Average Model	
		ARC 2	ARC 4	ARC 2	ARC 4	ARC 2	ARC 4	ARC 2	ARC 4	ARC 2	ARC 4
Average measured irradiance, mw/cm²	H	116 6	117.8	116 6	117 8	116.6	117.8	116 6	117 8	116 6	117 8
Standard deviation of H, mw/cm²	$S(H)$	±0 3	±0 2	±0 3	±0 2	±0.3	±0 2	±0 3	±0.2	±0 3	±0.2
Quartz-window transmittance	τ_w	0 8958	0 9004	0 8946	0 8993	0.8944	0 8990	0.8937	0.8983	0 8945	0 8990
Solar irradiance at 25 km, mw/cm²	H_{25}	130.1	130 8	130 3	131 0	130.4	131.0	130.5	131.1	130.4	131.0
Atmospheric transmittance	τ_A	0 9751	0 9753	0 9735	0 9737	0.9766	0.9767	0 9744	0 9746	0.9763	0.9765
Solar radius vector, AU	R	1.01177	1.01177	1.01177	1 01177	1 01177	1.01177	1 01177	1 01177	1 01177	1.01177
Solar constant, mw/cm²	H_0	136.6	137 2	137 0	137 6	136.6	137.2	137 0	137 7	136 6	137.3
Solar spectral model solar constant, mw/cm²	H_{0m}	139 0	139 0	139 0	139 0	136 6	136 6	135.1	135.1	136 7	136.7
Deviation of model H_{0m} from measured H_0, %	δH_{0m}	+1.7	+1 3	+1.4	+1 0	±0.0	−0.4	−1 4	−1.9	+0 1	−0 4
Averaged solar constant (each model), mw/cm²	$\langle H_0 \rangle$	136 9		137 3		136 9		137.4		137 0	
Deviation of H_{0m} from H_0, %	$\delta H_{0m}'$	+1 5		+1.2		−0 2		−1 7		−0.2	

various solar-spectral models used are shown in Table 5. The last spectral model is an average of the first four, each weighted by the square of the reciprocal of $\delta H_0'_m$ (see equation 19).

The ninth entry in Table 5 is the integrated irradiance of each model, or the model solar constant (H_{0_m}). The deviation of H_{0_m} from the solar constant computed by using the ACR measurements (H_0) is defined as

$$\delta H_{0_m} = [1 - \langle H_0/H_{0_m}\rangle] \quad (18)$$

The averaged solar constant $\langle H_0\rangle$ for each model is equal to $(H_{0_2} + H_{0_4})/2$. The deviation of H_{0_m} from the observed $\langle H_0\rangle$ is $\delta H_0'_m$

$$\delta H_{0_m}' = [1 - (\langle H_0\rangle/H_{0_m})] \quad (19)$$

Absolute Uncertainty of the ACR II Solar-Constant Results

Computation of the uncertainty of the ACR solar-constant value relative to the absolute radiometric scale follows the method of the second section. Most of the parametric quantities listed in Table 1 are the same for ACR 2 and ACR 4 and apply to both the Table Mountain tests and the balloon flight. The quantities that are not the same are listed in Table 6. The uncertainty in the cavity heater voltage is larger than the uncertainty for the Table Mountain comparisons owing to telemetry limitations The increased uncertainty in τ_w is due to the contamination problem discussed previously. The uncertainty in the solar-constant value must include the uncertainties of H, τ_w, τ_A, and R in a combination dictated by the form of equation 17. Table 7 contains these quantities and their uncertainties. The net uncertainty in H_0 is found to be ± 2.8 mw/cm^2 for ACR 2 and ± 2.2 mw/cm^2 for ACR 4. The solar-constant values on the ACRS, derived from the measurements of ACR's 2 and 4 in the 1968 balloon-flight experiment and reported relative to the weighted average spectral model, are

$$H_{0_2} = 136.6 \pm 2.8 \text{ mw/cm}^2 \quad (20)$$

$$H_{0_4} = 137.3 \pm 2.2 \text{ mw/cm}^2 \quad (21)$$

OTHER MEASUREMENTS

There have been numerous other high-altitude solar-constant measurements made in recent years by using both balloons and aircraft as the experimental platform. Attention will be limited here to observations made well above the tropopause, since the variability of atmospheric water vapor and aerosols considerably degrades the accuracy of total irradiance measurements at lower altitudes.

Measurements of total solar irradiance from high-altitude balloons (25- to 33-km peak altitudes) have been made since 1961 by scientists of the University of Leningrad [*Kondratiev and Nikolsky,* 1970]. They report a solar-constant value of 135.3 mw/cm^2 on the international pyrheliometric scale. A similar series of measurements, using high-altitude balloons in the same range of altitudes, has been performed by a team of experimenters from the University of Denver [*Murcray et al.,* 1968]. The reported value of the solar constant, $H_0 = 133.4$ mw/cm^2, is also referenced to the IPS. The NASA X-15 high-altitude research aircraft was the platform for another IPS-referenced measurement of the solar constant in 1967 [*Laue et al.,* 1968]. From the data taken at altitudes in excess of 80 km a solar-constant value of 136.0 mw/cm^2 was derived.

These three experiments had several important features in common: (*a*) they used thermopile-type relative (as distinguished from absolute) detectors as flight instruments; (*b*) the reported values of the solar constant were re-

TABLE 6. Parameters of the Balloon-Flight ACR's

Parameter	Symbol	ACR 2		ACR 4	
		Value	Uncertainty	Value	Uncertainty
Cavity aperture area, cm^2	A_c	1.0128	± 0.0018	1.0101	± 0.0027
Annulus area, cm^2	A_a	0.0118	± 0.0025	0.0150	± 0.0032
Cavity heater resistance, ohms	R_c	648.8	± 0.5	660.0	± 0.5
Cavity heater voltage, volts	V_c, V_0	0–25	± 0.025	0–25	± 0.025

TABLE 7. Parameters and Uncertainties for Computing the Solar Constant

Quantity		ACR 2		ACR 4	
		Value	Uncertainty	Value	Uncertainty
H_o	mw/cm²	116.6	±0.871	117.8	±0.940
R_o	AU	1.01177	$\pm 25 \times 10^{-6}$		
τ_w		0.8945	±0.0166	0.8990	±0.0122
τ_A		0.9763	±0.0024	0.9765	±0.0024

ferenced to the IPS; (*c*) the IPS calibrations were made on the ground by using the sun as a source and comparing thermopile output to irradiance measured by angstrom pyrheliometers.

Measurements of the solar constant were made outside the earth's atmosphere by instruments on board the NASA Mariner 1969 spacecraft [*Plamondon,* 1969]. The instruments, referred to as thermal control flux monitors (TCFM's), are nearly identical to the ACR I, an early form of the ACR II. The TCFM is not used as a standard detector, however, but it is calibrated with reference to a blackbody radiation source. This fact may explain the difference between the reported TCFM solar-constant value of $H_o = 135.25$ mw/cm² and the ACR II balloon-flight value.

CONCLUSIONS

Analysis indicates that the ACR II is capable of defining the absolute radiometric scale with an uncertainty of less than ±0.5% under the conditions of the Table Mountain ACRS-IPS comparison tests. The necessary element for the Table Mountain accuracy was the direct determination during the test of the ACR effective quartz-window transmittance. The larger uncertainty of the balloon-flight measurements was primarily due to the quartz-window contamination problem.

The 2.2% ACRS-IPS difference exceeds the absolute uncertainty of the ACRS and is positive. Irradiance measurements on the IPS, as defined by Eppley-Angstrom 8420, are systematically low relative to the ACRS by from −1.7 to −2.7%. The scale difference does not appear to be due to differing solar-aureole effects on the ACR II and Eppley-Angstrom pyrheliometer under the conditions of the Table Mountain tests.

The 1968 ACR II balloon-flight experiment represents the first direct measurement of solar irradiance by standard detectors at an altitude where extinction by atmospheric water vapor and known aerosol distributions are negligible. The mean solar constant on the ACRS, based on the 1968 flight, is $H_o = 137.0$ mw/cm² with an absolute uncertainty of less than ±2%.

Acknowledgments. This work presents the result of one phase of research conducted at the Jet Propulsion Laboratory, California Institute of Technology, under contract NAS 7-100, sponsored by the National Aeronautics and Space Administration.

* * *

The Editor wishes to thank A. J. Drummond and D. G. Murcray for their assistance in evaluating this paper.

REFERENCES

Angstrom, A., and B. Rhode, Pyrheliometric measurements with special regard to the circumsolar sky radiation, *Tellus, 18*(1), 25, 1966.

Arvesen, J. C., et al., Determination of extraterrestrial solar-spectral irradiance from a research aircraft, *J. Appl. Opt., 8,* 2215, 1969.

Crommelynk, D., and R. Dongniaux, An absolute scale for radiation measurement, *Paper 3143,* presented at the International Solar Energy Society Conference, Melbourne, Australia, 1970.

Elterman, L., *Handbook of Geophysics and Space Environments,* chap. 7, pp. 7-14–7-35, Macmillan, New York, 1965.

Gast, P. R., *Handbook of Geophysics and Space Environments,* chap. 16, p. 16-1, Macmillan, New York, 1965.

Haley, F., A rapid-response blackbody cavity radiometer, *JPL New Tech. Rep. 30-521,* Jet Propulsion Laboratory, Pasadena, Calif., 1964.

Houghton, J., The absorption of solar infrared radiation by the lower stratosphere, *Quart. J. Roy. Meteorol. Soc., 89,* 319, 1963.

Kendall, J. M., Sr., The JPL standard total-radiation absolute radiometer, *JPL Tech. Rep. 32-1263,* Jet Propulsion Laboratory, Pasadena, Calif., May 5, 1968.

Kendall, J. M., Sr., Primary absolute cavity radiometer, *JPL Tech. Rep. 32-1396,* Jet Propulsion Laboratory, Pasadena, Calif., July 15, 1969.

Kendall, J. M., and C. M. Berdahl, Two blackbody radiometers of high accuracy, *J. Appl. Opt., 9,* 1082, May, 1970.

Kondratiev, K. Ya., and G. A. Nikolsky, Solar radiation and solar activity, *Quart. J. Roy. Meteorol. Soc., 96,* 509, 1970.

Labs, D., and H. Neckel, The radiation of the solar photosphere from 2000 to 100μ, *Z. Astrophys., 69,* 1–73, 1968.

Laue, E., G., and A. J. Drummond, Solar constant, first direct measurements, *Science, 161,* 888–891, 1968.

Murcray, D. G., T. G. Kyle, J. J. Kosters, and P. R. Gast, The measurements of the solar constant from high-altitude balloons, *Tellus, 21,* 620–624, 1969.

Plamondon, J. A., The Mariner 1969 temperature control flux monitor, *Space Programs Summary 37–59,* vol. 3, 162, Jet Propulsion Laboratory, Pasadena, California, 1969.

Plamondon, J. A., and J. M. Kendall, Sr., A cavity-type, absolute, total-radiation radiometer, in *Space Programs Summary 37–35,* vol. 4, Jet Propulsion Laboratory, Pasadena, Calif., September 13, 1965.

Schöne, W., Results of pyrheliometer comparisons made in Potsdam with regard to recent investigations on the influence of circumsolar sky radiation, paper presented at Precision in Pyrheliometric Measurements Seminar, Brussels, 1966.

Sparrow, E. M., Radiation heat transfer between surfaces, *Advanced Heat Transfer,* vol. 2, edited by James P. Hartnett and Thomas F. Irvine, Jr., p. 400, 1965.

Sparrow, E. M., and V. K. Jonsson, Radiant emission characteristics of diffuse conical cavities, *J. Opt. Soc. Am., 53,* 816, 1963.

Syndor, C., A numerical study of cavity radiometer emissivities, *JPL Tech. Rep. 32-1463,* Jet Propulsion Laboratory, Pasadena, Calif., February 15, 1970.

Thekaekara, M. P., R. Kruger, and C. H. Duncan, Solar irradiance measurements from a research aircraft, *J. Appl. Opt., 8,* 1713, 1969.

Willson, R. C., Experimental and theoretical comparison of the JPL active cavity radiometric scale and the international pyrheliometric scale, *JPL Tech. Rep. TR 32-1365,* Jet Propulsion Laboratory, Pasadena, Calif., February 1, 1969.

(Received October 9, 1970;
accepted March 4, 1971.)